Quaternary Science Reviews 150 (2016) 55–66

Contents lists available at ScienceDirect

Quaternary Science Reviews

journal homepage: www.elsevier.com/locate/quascirev

# Long-term record of Barents Sea Ice Sheet advance to the shelf edge from a 140,000 year record

Ed L. Pope [a, *], Peter J. Talling [a, b], James E. Hunt [a], Julian A. Dowdeswell [c], Joshua R. Allin [a], Matthieu J.B. Cartigny [a], David Long [d], Alessandro Mozzato [a], Jennifer D. Stanford [e], David R. Tappin [d], Millie Watts [a]

[a] National Oceanography Centre, Southampton, European Way, Southampton, SO14 3ZH, UK
[b] Departments of Earth Science and Geography, University of Durham, Durham, DH1 3LE, UK
[c] Scott Polar Research Institute, University of Cambridge, Lensfield Road, Cambridge, CB2 1ER, UK
[d] British Geological Survey, Keyworth, NG12 5GG, UK
[e] Department of Geography, University of Swansea, SA2 8PP, UK

ARTICLE INFO

*Article history:*
Received 19 May 2016
Received in revised form
4 August 2016
Accepted 9 August 2016

*Keywords:*
Glacigenic debris-flows
Ice sheet
Ice stream
Trough-Mouth Fan
Weichselian
Barents Sea Ice Sheet
Sedimentary records

ABSTRACT

The full-glacial extent and deglacial behaviour of marine-based ice sheets, such as the Barents Sea Ice Sheet, is well documented since the Last Glacial Maximum about 20,000 years ago. However, reworking of older sea-floor sediments and landforms during repeated Quaternary advances across the shelf typically obscures their longer-term behaviour, which hampers our understanding. Here, we provide the first detailed long-term record of Barents Sea Ice Sheet advances, using the timing of debris-flows on the Bear Island Trough-Mouth Fan. Ice advanced to the shelf edge during four distinct periods over the last 140,000 years. By far the largest sediment volumes were delivered during the oldest advance more than 128,000 years ago. Later advances occurred from 68,000 to 60,000, 39,400 to 36,000 and 26,000 to 20,900 years before present. The debris-flows indicate that the dynamics of the Saalian and the Weichselian Barents Sea Ice Sheet were very different. The repeated ice advance and retreat cycles during the Weichselian were shorter lived than those seen in the Saalian. Sediment composition shows the configuration of the ice sheet was also different between the two glacial periods, implying that the ice feeding the Bear Island Ice stream came predominantly from Scandinavia during the Saalian, whilst it drained more ice from east of Svalbard during the Weichselian.



## 1. Introduction

High-latitude continental shelves have experienced multiple glacial advance and retreat cycles during the Quaternary (Dowdeswell et al., 1998; Ó Cofaigh et al., 2003; Svendsen et al., 2004a; Winsborrow et al., 2012; Patton et al., 2015). The ice dynamics and retreat of the Late Weichselian (29,000–14,000 years Before Present) ice sheets are quite well constrained because relatively well-preserved and dated sediments (Sættem et al., 1994; Vorren and Laberg, 1997; Landvik et al., 1998; Solheim et al., 1998) and submarine geomorphology (Ottesen et al., 2005; Andreassen et al., 2008; Winsborrow et al., 2010, 2012) allow reconstruction of ice sheet history. However, the most recent glacial advance and retreat reworked earlier sediments and overprinted older geomorphology, thereby obscuring the record of past ice behaviour. It is therefore difficult to reconstruct the timing of advance and retreat cycles and ice stream dynamics beyond the Late Weichselian (Ingólfsson and Landvik, 2013; Patton et al., 2015). An exception to this is the archive of continental-slope sediments which make up trough-mouth fans.

Trough-Mouth Fans are found at the outer margins of bathymetric cross-shelf troughs which extend across the continental shelf to the shelf edge (Batchelor and Dowdeswell, 2014). During full-glacial periods, these cross-shelf troughs are frequently filled by ice streams, which are curvilinear areas of fast-flowing ice that are critical to dynamics and stability of ice sheets (Ó Cofaigh et al., 2003; Schoof, 2007). Where ice streams overlie deformable sedimentary beds, exceptionally large volumes of debris can be transferred across the continental shelf (Dowdeswell and Siegert, 1999;

* Corresponding author.
*E-mail address:* Ed.Pope@noc.soton.ac.uk (E.L. Pope).

http://dx.doi.org/10.1016/j.quascirev.2016.08.014

Ó Cofaigh et al., 2003; Dowdeswell et al., 2010). Once deposited at the shelf edge, the glacial sediment is re-mobilised on the upper continental slope and redeposited by gravity-flow processes to form a Trough-Mouth Fan (Vorren et al., 1998; Nygard et al., 2005; Nygård et al., 2007). Sedimentary deposits that make up trough-mouth fans are therefore a potentially valuable long-term record of ice streams and their dynamics. This study focusses on the sedimentary record contained in the Bear Island Trough-Mouth Fan.

### 1.1. Regional setting

The Bear Island Trough-Mouth Fan is situated beyond the Bear Island cross-shelf trough (Fig. 1). The trough is about 150 km wide and 500 m deep at its mouth and served as a major drainage pathway for the Barents Sea Ice Sheet. The Bear Island Trough-Mouth Fan covers an area of 215,000 $km^2$ and has a volume of approximately 395,000 $km^3$ (Vorren and Laberg, 1997; Taylor et al., 2002a, 2002b). It is one of the largest sediment accumulations on Earth, with a volume comparable to submarine fans developed offshore of the World's largest rivers. Sediment accumulation here is episodic and its rate can be an order of magnitude greater than is seen on river-fed systems (Dowdeswell et al., 2010).

The Bear Island Trough-Mouth Fan extends from the continental shelf edge at water depths of ~500 m to over 3000 m in the Lofoten Basin (Fig. 1). The most recently active (Late Weichselian) part of the Bear Island Trough-Mouth Fan is at the northern end of the fan and covers ~125,000 $km^2$ (Taylor et al., 2002a, 2002b). Here, side-scan sonar mapping revealed a series of low backscatter, debris-flow lobes that radiate out from the top of the fan with runout distances of up to 490 km (Fig. 1; Laberg and Dowdeswell, 2016). Each of these numerous debris-flows is estimated to have remobilised ~15–20 $km^3$ of sediment. They are also thought to indicate the presence of ice at (or close to) the shelf edge (Vorren and Laberg, 1997; Taylor et al., 2002a). However, no previous study has dated a long record of stacked debris-flows on the Bear Island Trough-Mouth Fan due to the thickness of these debris-flow deposits (Laberg and Vorren, 1995).

In this study we demonstrate a novel methodology for understanding the growth and decay of ice streams by dating the times at which the Bear Island Ice stream was at the shelf edge. This is achieved using muddy distal deposits on the lower part of the Bear Island Trough-Mouth Fan beyond glacigenic debris-flows higher up the continental slope (Figs. 1 and 2).

### 1.2. Aims

Our aim is to address the following questions. First, can multiple glacigenic debris-flows on the Bear Island Trough-Mouth Fan be dated and can they be used to reconstruct a history of the advance and retreat of the Barents Sea Ice Sheet? Secondly, did the dynamics of the Barents Sea Ice Sheet vary between different advance and retreat cycles and can this information be elicited from glacigenic debris-flow deposits? As an example, does the lithofacies or geochemical composition of glacigenic debris-flows vary? Last, can we use glacigenic debris-flows to help understand the controls on marine-based ice sheet retreat?

## 2. Material and methods

The principal data source for this paper is a suite of gravity cores collected during cruise 64PE391 of the RV *Pelagia* to the Norwegian Sea in 2014. These cores are supplemented by gravity cores collected during cruises JR51 and JR142 of the RRS *James Clark Ross* in 2000 and 2006 respectively (Table 1). In addition, the paper uses geophysical data collected during cruises of the RV *Pelagia* in 2014 and RRS *James Clarke Ross* in 2000. These data comprise 3.5 kHz sub-bottom profiler records and 6.5 kHz GLORIA side-scan sonar imagery with a swath width of about 20 km.

### 2.1. Core logging

Cores were logged visually, identifying colour, facies and grain size. Cores were also analysed using a Geotek MSCL core logger for p-Wave velocity, gamma-ray density and magnetic susceptibility. Measurements were taken at a 0.5 cm resolution. X-radiographs of cores PE73 and PE75 were taken using an ITRAX μXRF core scanner. X-radiograph conditions were 60 kV and 45 mA, with a dwell time of 400 ms, at a resolution of 200 μm (Croudace et al., 2006).

### 2.2. Dating

#### 2.2.1. Radiocarbon dating

Monospecific samples of the planktonic foraminifera *Neogloboquadrina pachyderma* sinistral from PE73 and PE75 were dated by Accelerator Mass Spectrometry (AMS). The radiocarbon ages were converted to calibrated ages (Cal years BP) using the Marine 13 database (Reimer et al., 2013).

#### 2.2.2. Coccolithophore biostratigraphy

To provide accurate and robust datum horizons beyond radiocarbon dating, coccolithophore biostratigraphy was used. Toothpick hemipelagite samples were taken, from which species abundance counts were made. Species present were counted using a *Hitachi TM1000 SEM* which enabled high resolution (1000–10,000×) images to be taken. The species present in each sample were counted for abundance across 10 fields of view on the *SEM* at a magnification of 2000.

These abundance counts were then compared to coccolith abundances that had previously been made by Gard (1988) and Backman et al. (2009). These two studies demonstrated that abundances of *Emiliania huxleyi, Gephyrocapsa mullerae, Gephyrocapsa caribbeanica, Gephyrocapsa apperta, Calcidiscus leptoporus* and *Coccolithus pelagicus* could be calibrated to oxygen isotope stages in the polar North Atlantic. Each datum horizon is outlined in Table 2 and Fig. 3.

#### 2.2.3. ITRAX μXRF geochemistry

ITRAX μXRF was used to collect high resolution (1 mm) major element geochemical records from four cores. Cores PE73, PE75, GC08 and JR142 were analysed using this method. Proxy dating was achieved by removing glacigenic debris-flow deposits from the cores to leave the hemipelagite μXRF records. The hemipelagite calcium (Ca) record was used as a proxy for $\delta^{18}O$ as changes should be primarily driven by changes to biogenic $CaCO_3$ production which is affected by changing surface water conditions, changing circulation patterns and sea level (Richter et al., 2001; Cheshire et al., 2005; Croudace et al., 2006; Rothwell et al., 2006; Lebreiro et al., 2009; Hibbert et al., 2010; Solignac et al., 2011; Hunt et al., 2013). Located on the distal areas of the Bear Island Trough-Mouth Fan, hemipelagite composition should therefore reflect open water conditions. The μXRF calcium record, combined with AMS dating and the Coccolith biostratigraphy enables a robust chronology of glacigenic debris-flows on the fan to be constructed.

### 2.3. Dating glacigenic debris-flows

Dating of glacigenic debris-flows on the Bear Island Trough-Mouth Fan was achieved in the upper part of the core using $^{14}C$ AMS dates. Average hemipelagic accumulation rates between

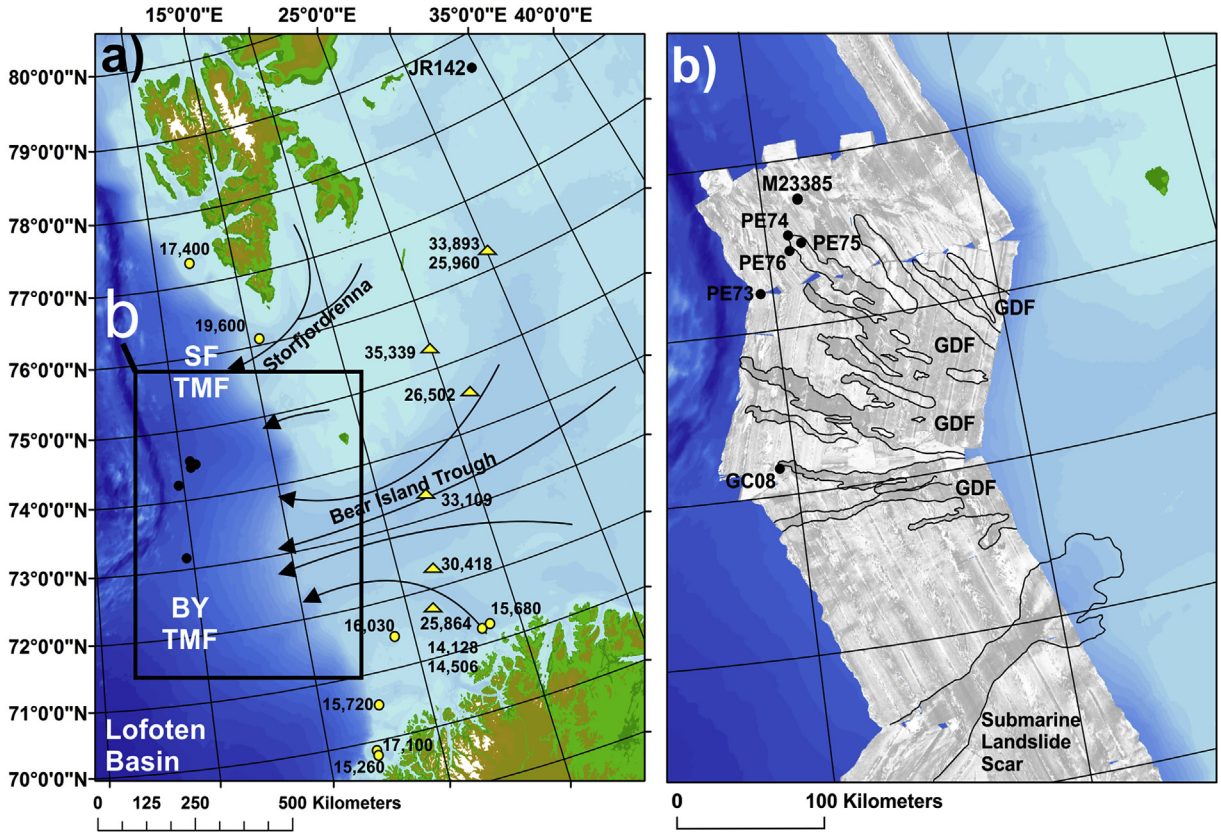


**Fig. 1.** Regional setting of the Bear Island Trough-Mouth Fan. a) Core locations (black dots) shown with respect to Last Glacial Maximum ice flow direction inferred from the orientation of streamlined seafloor bedforms (Winsborrow et al., 2010). SF TMF = Storfjorden Trough-Mouth Fan. BY TMF = Bear Island Trough-Mouth Fan. Yellow triangles show dates from till units giving maximum age estimates for the onset of the last glacial advance and dots triangles show dates from glaciomarine sediments giving minimum estimates for the onset of deglaciation (Winsborrow et al., 2010). b) Bear Island Trough-Mouth Fan with GLORIA long range side-scan sonar imagery – superimposed. Core positions are labelled. Glacigenic debris-flows (GDF) and the Bjørnøya submarine landslide are identified using the GLORIA imagery. (For interpretation of the references to colour in this figure legend, the reader is referred to the web version of this article).

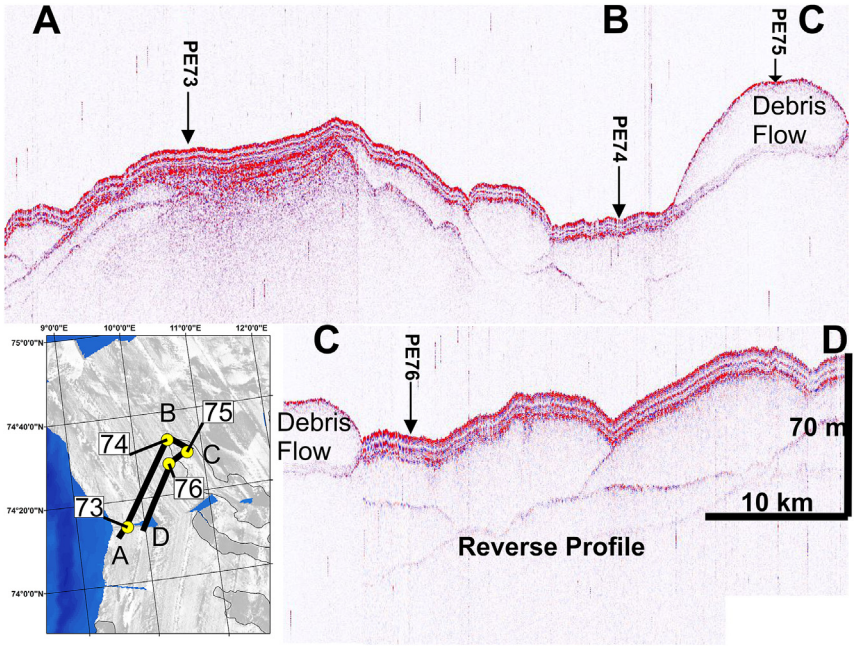


**Fig. 2.** 3.5 kHz seismic profile across the distal Bear Island Trough-Mouth Fan between core locations. The most recent glacigenic debris-flow, where PE75 is situated, is shown to have very little drape. Other glacigenic debris-flows are found beneath multiple reflectors. From this we suggest that the glacigenic debris-flows identified from the GLORIA imagery represent the glacigenic debris-flows which occurred during the Late Weichselian glacial advance to the shelf edge of the Bear Island Trough. The glacigenic debris-flows found deeper, beneath multiple reflectors are from older glacial advances, probably originating during or before the Saalian glacial advance to the shelf edge.

**Table 1**
Site information for sediment cores. Core locations are shown in Fig. 1.

| Core name | Latitude | Longitude | Water depth (m) | Length (cm) |
|---|---|---|---|---|
| PE73 | 74°12.30′N | 09°40.49′E | 2440 | 916 |
| PE74 | 74°33.12′N | 10°34.55′E | 2465 | 821 |
| PE75 | 74°29.01′N | 10°49.38′E | 2416 | 377 |
| PE76 | 74°27.52′N | 10°32.07′E | 2403 | 798 |
| GC08 | 73°10.00′N | 09°40.00′E | 2289 | 320 |
| JR142 | 78°34.07′N | 34°03.40′E | 212 | 100 |

radiocarbon dates were calculated and then the hemipelagic depth between the deposits was used to calculate the timing of the emplacement of the deposits (Wetzel, 1984; Hunt et al., 2013; Clare et al., 2014). To do this, we assumed that flows were not erosional and that the rate of sedimentation between radiocarbon dates was constant. Beyond the depth which we could use radiocarbon ages we used tie points in the coccolith biostratigraphy (Weaver and Kuijpers, 1983; Weaver et al., 1992; Hunt et al., 2013) and the calcium proxy curve (Hibbert et al., 2010) to estimate the rate of hemipelagite accumulation and thus the timing of the events.

#### 2.3.1. Statistical analysis of glacigenic debris-flow recurrence

In order to try to identify the possible triggering mechanism for glacigenic debris-flows on the Bear Island Trough-Mouth Fan the distribution of recurrence intervals was analysed. Here, we define the recurrence interval of a glacigenic debris-flow as the length of time since the glacigenic debris-flow that preceded it. Previous work has identified sediment gravity-flows to be temporally random, i.e. their recurrence intervals followed a Poisson distribution, meaning no precise triggering mechanism could be identified (Clare et al., 2014; Pope et al., 2015). However, these studies suggest that the use of statistical tests on recurrence intervals at local, rather than on regional or global datasets as they used, may provide insight into the triggering mechanisms of submarine sediment gravity-flows (Pope et al., 2015).

To assess whether the recurrence intervals between glacigenic debris-flows come from a Poisson distribution or a different statistical distribution we used the Anderson-Darling test. The Anderson-Darling test is defined as:

$$A^2 = -N - S \tag{1}$$

where

$$S = \sum_{i=1}^{N} \frac{(2i-1)}{N} [lnF(Y_i) + \ln(1 - F(Y_{N+1-i}))] \tag{2}$$

$F$ is the cumulative distribution function of the specific distribution. The test was carried out on 47 recurrence intervals on core PE73.

In addition to the Anderson-Darling test, we also analysed the degree of clustering of the recurrence intervals. The degree of clustering of low and high values of recurrence within the sequence was analysed using a rescaled range exponent which was developed by Hurst (1951). Hurst (1951) presented the following relationship, using $K$ as an estimator for a modified Hurst Exponent, h:

$$K = \frac{\log_{10}(R/S)}{\log_{10}(N/2)} \tag{3}$$

where $R$ is the maximum range in cumulative departure from the mean, $N$ is the number of observations, and $S$ is the standard deviation (Chen and Hiscott, 1999). Values that are closer to $K = 1$ show persistent or trend reinforcement (i.e. a large value is most likely followed by a large value; Mandelbrot and Van Ness, 1968) and those that are closer to $K = 0$ are mean reverting or anti-persistent (i.e. a large value is most likely followed by a small value; Barkoulas et al., 2000). Values that approximate $K = 0.5$ are deemed to be randomly distributed.

### 2.4. Geochemical composition of the glacigenic debris-flows

To analyse the geochemical composition of the glacigenic debris-flows the mud fraction was first grain-sized. Sediment samples of 1 $cm^3$ were added to 30 mL RO water with a 0.05% sodium hexametaphosphate dispersant and shaken for a minimum of 12 h. The dispersed sediment mixtures were then analysed using a *Malvern Mastersizer 2000* particle size analyser. Standard reference (SRM) of mean average 32 μm and 125 μm was used to monitor accuracy.

Once comparable sample deposits from the glacigenic debris-flows were identified in terms of similar grain sizes their major element records produced by the ITRAX μXRF scanner were compared. Both single element records and major element ratios were compared.

## 3. Results

### 3.1. Glacigenic debris-flow sedimentary characteristics

Cores PE73, PE74, PE75 and PE76 were located several hundred kilometres from the palaeo-ice front on the Bear Island Trough-Mouth Fan at water depths in excess of 1750 m (Fig. 1). In such distal locations, the downslope evolution of glacigenic debris-flows (Ó Cofaigh et al., 2003) results in the deposition of fine muds. We henceforth refer to these fine-mud deposits as distal debris-flow muds.

**Table 2**
Coccolithophore biostratigraphy zonation scheme for the Lofoten Basin; from Gard (1988).

| Age (ka) | OIS stage | Abundance | Description |
|---|---|---|---|
| 0–8 | Recent – mid/lower 1 | High | Assemblage is dominated by *C. pelagicus* and *E. huxleyi*. *Calcidiscus leptoporus* and *Gephyrocapsa* spp. are present in low numbers. Rare specimens of *Helicosphaera carteri*. Lower boundary usually coincides with the end of the last barren interval. |
| 8–66 | Mid/lower 1 – mid 4 | Mainly barren | Interval is mainly barren of nanno-fossils but thin horizons with some *E. huxleyi* and *Gephyrocapsa* spp. are occasionally present. |
| 66–79 | Mid 4–5a | High | *Gephyrocapsa mullerae* and *E. huxleyi* show abundance peaks. Both *G. caribbeanica* and *C. pelagicus* are present. |
| 79–97 | 5b–5d | Low | Assemblage is almost exclusively composed by *Gephyrocapsa* spp. with some *E. Huxleyi*. In some cases in northerly areas this is partly or completely barren. |
| 97–119 | Upper 5e | High | Total amount of nanofossils forms an abundance peak in this subzone. Dominated by *Gephyrocapsa mullerae* and *E. Huxleyi* with abundance peak of *C. leptoporus*. |
| 119–280 | Lowermost 5 – lowermost 8 | Mainly barren | Low amounts of nannofossils occur. Assemblage dominated by *Gephyrocapsa aperta*. Minor numbers of *C. pelagicus*, *E. Huxleyi* and *C. leptoporus* may also be present. |

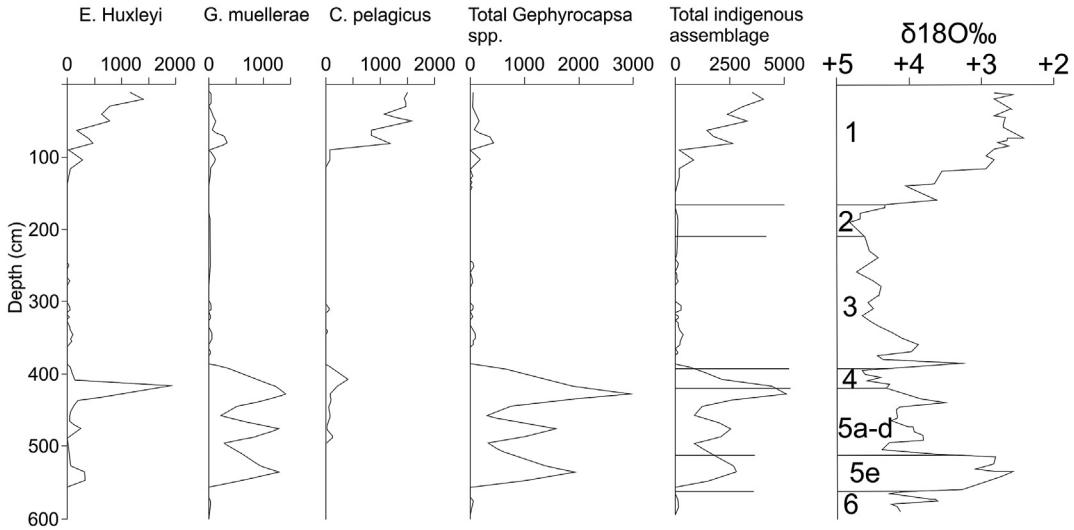


**Fig. 3.** Abundances of calcareous nannofossils from Norwegian Sea Core V27-60 (78°11N, 8°35E). Oxygen isotope stratigraphy is taken from Labeyrie and Duplessy (1985). Figure is adapted from Backman et al. (2009).

Cores PE73, PE74 and PE76 contained 59, 42 and 38 thin fine-mud layers, respectively, which originated from glacigenic debris-flows further upslope. Located furthest from the shelf edge, the largest number of distal debris-flow mud layers are found in core PE73 (Fig. 4). These deposits are mainly dark grey muds; their grain size distribution is 55% mud (<1–10 microns), 24% silt (10–62.5 microns) and 21% sand (62.5 > 2000 microns) (Fig. 5). These deposits have sharp basal contacts and higher average grainsizes than the background sediments (67% mud, 19% silt, 12% sand). Deposits in cores PE74 and PE76 have similar characteristics. However, the bottom-most sediments in these two cores are massive glacigenic debris-flow deposits (diamictons; see Fig. 5c) described elsewhere in the literature (Vorren et al., 1991; Vorren and Laberg, 1997; Taylor et al., 2002a, 2002b; Ó Cofaigh et al., 2003). The diamictons consist of lithic clasts supported by an unsorted dark sand-mud matrix (39% mud, 32% silt, 27% sand).

Core PE75 was located on what is the youngest glacigenic debris-flow in the study area stratigraphically and contained three sediment-flow deposits. Two were distal debris-flow muds seen in cores PE73, PE74 and PE76. The largest deposit was composed of a massive diamicton (Figs. 5c and 6). The cross core correlation illustrated in Fig. 7 shows how the thick glacigenic debris-flow in the base of PE75 is laterally equivalent to the thin mud layers seen in PE73, PE74 and PE76 more distally on the trough-mouth fan. We use this to justify our use of the thinner distal debris-flow muds as representative of glacigenic debris-flow occurrence further upslope.

### 3.2. Timing and frequency of glacigenic debris-flows

The most recent distal debris-flow mud layer in PE75 dates to <11,000 Calibrated years Before Present (Cal BP), and its timing is consistent with dated glacigenic debris-flows from other studies (Laberg and Vorren, 1996). The large glacigenic debris-flow deposit at the base of core PE75 dates to ~23,000 Cal BP. These deposits are consistent with the Late Weichselian glacial advance (Winsborrow et al., 2010, 2012; Patton et al., 2015). In core PE73, Late Weichselian distal debris-flow muds occur between 26,000 and 20,900 Cal BP. The radiocarbon dates and the cross-correlations (Figs. 7 and 8) show a consistent phase of deposition of these distal debris-flow mud layers across the Bear Island Trough-Mouth Fan during this period. The next group of distal debris-flow mud deposits in core PE73 date to between 39,400 and 36,000 Cal BP. The last set of distal debris-flow mud layers during the Weichselian were emplaced between 68,000 and 60,000 BP (Fig. 8). The largest number and greatest thickness of distal debris-flow mud deposits in core PE73 occurred earlier, during the Saalian glaciation with the youngest of these dated at ~128,000 BP (Fig. 8). The number and thickness of deposits from the Saalian also correlate well between cores PE74 and PE76 (Fig. 7).

#### 3.2.1. How do the core deposits relate to the seismic stratigraphy?

Dating of the glacigenic debris-flow at the base of PE75 (Fig. 6) and the cross-core correlations suggest that there is only a thin amount of hemipelagic drape over the most recent glacigenic debris-flows. The glacigenic debris-flow deposit at the base of PE75 can be seen in the seismic profile (Fig. 2) to only have a single overlying reflector and is also visible in GLORIA side-scan sonar (Figs. 1b and 2). We therefore suggest that the glacigenic debris-flows mapped using the GLORIA side-scan sonar imager and illustrated in Fig. 1b represent only those that occurred during the Late Weichselian glaciation. The other debris-flows visible in the seismic profiles as many reflectors beneath thicker sediment drapes (Fig. 2) thus date to earlier glacial advances.

#### 3.2.2. Is the clustering of glacigenic debris-flows supported statistically?

Visual inspection and cross-core correlations suggest that there are four apparent clusters of distal debris-flow muds on the northern end of the Bear Island Trough-Mouth Fan (Fig. 7). The significance of this clustering was tested by analysing the statistical distribution of recurrence intervals, the time between one event and the next, on deposits in core PE73. The Anderson-Darling Test and Hurst Exponent were applied to 47 recurrence intervals from PE73. The discrepancy between the 59 distal debris-flow muds in the core and the 47 recurrence intervals used is a result of the large number of deposits at the base of the core. These distal debris-flow muds have no hemipelagite between the events. We are therefore unable to calculate the time between events. Whilst this may be the result of large numbers of glacigenic debris-flows occurring over very short time intervals, we are unable to rule out the possibility that the hemipelagic sediment has been eroded. Consequently we

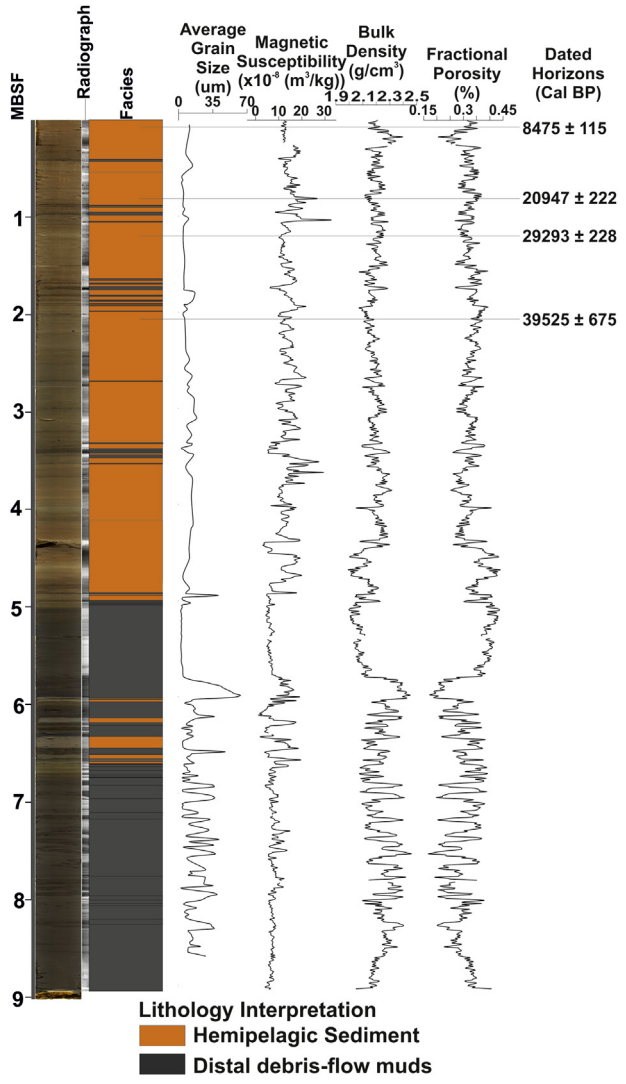


**Fig. 4.** Core panel for PE73. Panel includes core photos, x-radiographs of each core section, facies interpretation, average grain size, geophysical data and radiocarbon dates.

treat the multiple distal debris-flow muds at the bottom of the core as a single mass-transport complex.

Using the Anderson-Darling Test, the distribution of recurrence intervals most closely followed a 3-parameter Weibull distribution ($p > 0.5$; for the Anderson Darling Test to be significant at the 95% confidence interval the $p$ value must be >0.05). The recurrence intervals also had a Hurst's Exponent of 0.808. The statistical tests suggest that the distribution of distal debris-flow muds is therefore highly clustered rather than random; i.e. a short recurrence interval is likely to be followed by another short recurrence interval. These statistical tests suggest that the triggering of glacigenic debris-flows on the Bear Island Trough-Mouth Fan are probably related to a specific non-random process such as the presence of ice at the shelf edge.

### 3.3. Geochemical composition of distal debris-flow muds

The geochemical composition of the mud fraction of the flow deposits in cores PE73, PE75, GC08 and JR142 (Fig. 1) were analysed using ITRAX μXRF data. Ratios of major elements of the flow deposits were shown to have distinct differences (Fig. 9a). In core PE73 the ratios of the Weichselian distal debris-flow mud compositions were shown to be distinct from the Saalian deposits. Ratio data from the debris-flow deposits in PE75 matched the Weichselian deposits in PE73. This shows temporally similar deposits have the same composition at the northern end of the Bear Island Trough-Mouth Fan.

To identify whether the differences in deposit composition were a consequence of changes in provenance of the sediment, major element ratios from cores located in different areas of the Barents Sea and the Bear Island Trough-Mouth Fan (Fig. 1) were compared to the ratio data from cores PE73 and PE75. When ratio data from a distal debris-flow mud deposit in GC08 was compared to the ratios of deposits in PE73, it was shown to be similar to those of the Saalian distal debris-flow muds in PE73 (Fig. 9b). The geochemical ratio data from JR142, located east of Svalbard about 750 km north-east of the Bear Island Trough-Mouth Fan was, by contrast, shown to be similar to the Weichselian deposits in core PE73.

## 4. Discussion

### 4.1. How do reconstructions of past Barents Sea Ice Sheet advances compare to the timing of glacigenic debris-flow clusters?

Dating of the large glacigenic debris-flow deposit in core PE75 at ~23,000 Cal BP and the cluster of distal debris-flow muds in cores PE73, PE74 and PE76 (Fig. 7) between 26,000 and 20,900 Cal BP, is consistent with proposed dates for the initial advance to the shelf edge of the Late Weichselian Barents Sea Ice Sheet (Elverhoi et al., 1995; Laberg and Vorren, 1995; Vogt et al., 2001; Vorren et al., 2011). The timing is also contemporaneous with dated mass-transport deposits from trough-mouth fans offshore Western Svalbard (Dowdeswell and Elverhøi, 2002). In both areas, the ice retreated from the shelf edge as early as 20,000 Cal BP, inferred from a lack of younger glacigenic debris-flow deposits. Deposition of laminated mud and sand layers from meltwater plumes occurred at a later date as deglaciation accelerated and thus we see no evidence of this in our distally located cores (Jessen et al., 2010; Lucchi et al., 2013). The timing of this cluster of events, when ice was known to be at the shelf edge through independent radiocarbon dating of deposits (Fig. 1), and the statistical analysis (see Section 3.2.1.), validates the use of distal debris-flow mud deposits as an indicator of an ice advance to the shelf edge of the Bear Island Trough.

Assuming that each cluster of distal debris-flow muds represents an ice advance in the Bear Island Trough, earlier in the Weichselian ice reached the shelf edge between 39,400 and 36,000 Cal BP. An ice advance during this period is contrary to reconstructions made using terrestrial deposits on Svalbard (Mangerud et al., 1998; Svendsen et al., 2004b; Hughes et al., 2016). However, its timing is consistent with ice-rafted debris records from other dated cores on or near the Bear Island Trough-Mouth Fan (Dowdeswell et al., 1999; Dreger, 1999; Knies et al., 2001) and records of a glacial advance associated with the Jæren-Skjonghelleren advance in Scandinavia (Lambeck et al., 2010). The discrepancy between the Bear Island Trough-Mouth Fan records and those on Svalbard, 300 km to the north, can be explained through either: (1) a re-advance occurred on Svalbard; however, there are few terrestrial records of this advance on Svalbard; or (2) the response to climatic forcing of an ice dome east of Svalbard, and its outlet glaciers, which differs from that of glaciers on the archipelago itself.

The oldest Weichselian distal debris-flow muds occur between 68,000 and 60,000 BP. These are consistent with proposed glacial advances during Marine Isotope Stage 4 from terrestrial outcrops on Svalbard and ice-rafted debris records (Mangerud et al., 1998;

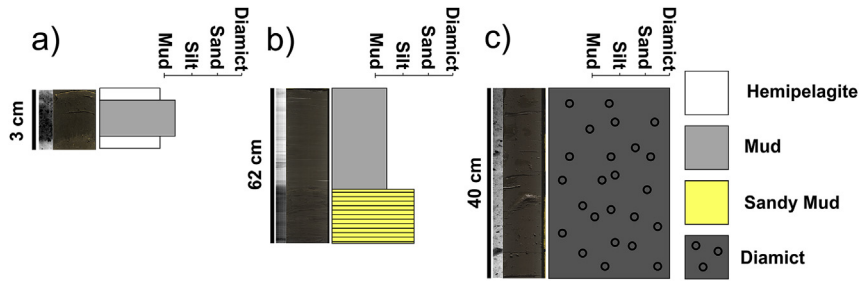


**Fig. 5.** Sedimentary logs and their radiographs that summarize the deposits seen in cores PE73, PE74, PE75 and PE76 related to glacigenic debris-flows. a) A typical distal debris-flow mud. b) Laminated sand underlying a distal debris-flow mud. c) A glacigenic debris-flow massive diamicton.

Svendsen et al., 2004a; Ingólfsson and Landvik, 2013). During Marine Oxygen Isotope Stage 5 (124–80,000 BP) the cores contain increased amounts of ice-rafted debris. There is, however, no evidence of distal debris-flow muds in the cores during Marine Oxygen Isotope Stage 5 (Figs. 7 and 8). We therefore propose that, whilst ice volumes increased in the Barents Sea, resulting in deposition of greater volumes of ice-rafted debris, the ice sheet did not reach the shelf edge of the Bear Island Trough at this time. This supports modelling studies of ice sheet growth for the Barents Sea during Marine Oxygen Isotope Stage 5 (Svendsen et al., 1999, 2004a, 2004b) and suggestions that the location of the largest ice dome migrated from east to west across the Barents-Kara Sea during each subsequent major glacial advance during the Weichselian (Siegert et al., 2001; Patton et al., 2015).

The presence of distal debris-flow muds occurring at >128,000 BP is consistent with reconstructions of the Late Saalian glacial maximum that occurred during Marine Isotope Stage 6 (Mangerud et al., 1998, 2001).

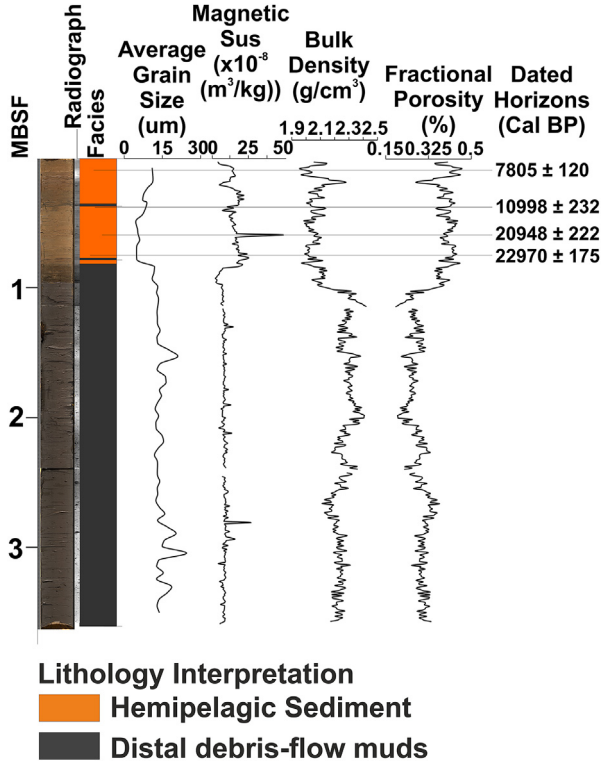


**Fig. 6.** Core panel for PE75. Panel includes core photos, X-radiographs of each core section, facies interpretation, average grain size, geophysical data and radiocarbon dates.

### 4.2. Contrasts between the Weichselian and Saalian Barents Sea Ice Sheets

#### 4.2.1. Ice-margin stability

The thickest and most numerous distal debris-flow mud deposits in cores PE73, PE74 and PE76 occur at the base of the cores. These deposits are dated biostratigraphically to >~128,000 BP (Fig. 8). If the number and thickness of distal debris-flow muds is representative of the volume of sediment advected to the shelf edge by the Bear Island Ice stream, then the duration or rate of sediment delivery was far greater during the Saalian than the Weichselian glacial interval. This could be explained by greater ice

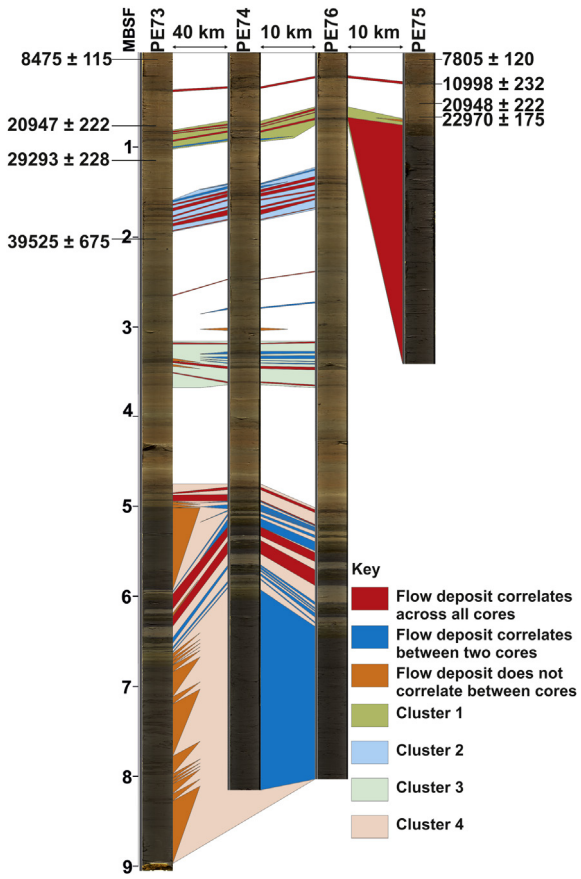


**Fig. 7.** Core correlations between cores PE73, PE74, PE75 and PE76. Distances between the cores and radiocarbon dates from cores PE73 and PE75 are shown. MBSF = Meters Below Sea Floor. Four clusters of distal debris-flow muds correlate well across the three long cores. Few deposits from glacigenic debris-flows occur outside of these main clusters.

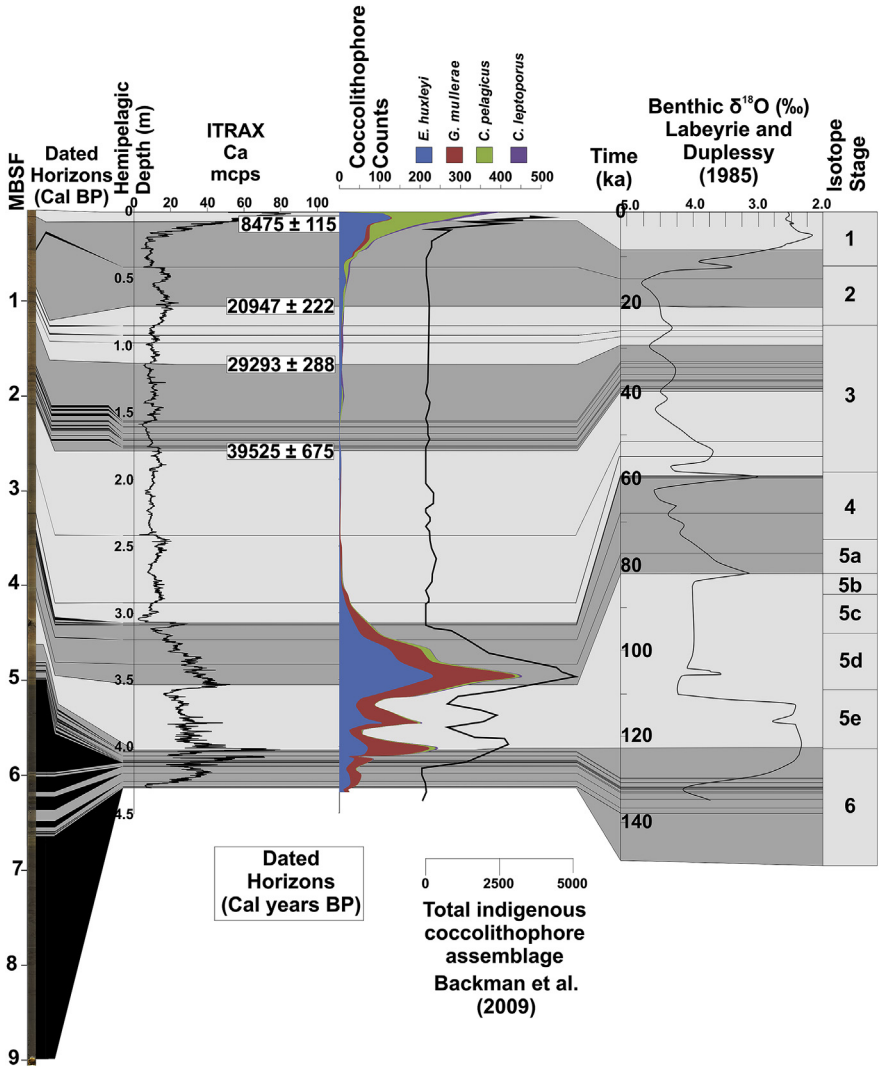


**Fig. 8.** Core panel for PE73 showing hemipelagic ITRAX Ca profile. Radiocarbon dates are initially used to correlate the core record with a local benthic $\delta^{18}O$ curve from core V27-60 offshore of the Bear Island Trough-Mouth Fan (Labeyrie and Duplessy, 1985). Beyond the range of radiocarbon dating, the ITRAX Ca profile is correlated with the $\delta^{18}O$ curve. Coccolithophore counts from toothpick hemipelagic samples are shown to corroborate the proxy dating using the ITRAX Ca profile based on the coccolith abundance curve from Backman et al. (2009) which was obtained from core V27-60.

thicknesses associated with the Late Saalian ice sheet leading to higher velocities, and an ice-front position stable at the shelf edge for a longer time period. This view is supported by model reconstructions of the Late Saalian ice sheet (Svendsen et al., 2004b; Colleoni et al., 2009), Arctic Ocean ice-rafted debris records (Spielhagen et al., 2004) and terrestrial records (Mangerud et al., 1998; Ehlers and Gibbard, 2004) indicating that the extent and duration of the Late Saalian ice sheet was greater than those which occurred during the Weichselian.

By comparison with the Saalian Barents Sea Ice Sheet, the Weichselian ice sheets produced comparatively few glacigenic debris-flows. Only four distal debris-flow muds were found in cores associated with the Late Weichselian advance. The two Middle Weichselian advances to the shelf edge were characterised by only 7 and 8 distal debris-flow mud deposits. The contrasts suggest that the time taken for ice sheet advance and retreat was shorter during the three (~ 26,000, 40,000 and 68,000 Cal BP) Weichselian glaciations, leading to smaller volumes of sediment reaching the shelf edge than during the (>128,000 BP) Saalian glaciation (Siegert et al., 2001).

*4.2.1.1. Ice-margin stability and rates of sediment delivery.* The following section briefly explores the implications of the newly dated ice stream advances and retreats for volumetric rates of sediment delivery to the Bear Island Trough-Mouth Fan, and thus for processes affecting the base of the ice stream.

Previous work suggests that around 4200 $km^3$ of sediment was supplied to the Bear Island Trough-Mouth Fan during the last glacial advance between 24,000 and 12,000 BP (Laberg and Vorren, 1996), although the exact volume is uncertain due to limitations in seismic coverage of the fan and dating uncertainties. However, even given the uncertainties, this is still a remarkably large volume of sediment. Subsequent modelling reconstructions have suggested that this sediment may have accumulated primarily during a period of about 13,000 years between 27,000 and 14,000 years BP (Dowdeswell and Siegert, 1999). This implied a sediment delivery rate of ~ 0.32 $km^3\ a^{-1}$ which is comparable to the annual sediment supply rate from the Amazon River (Milliman and Syvitski, 1992).

The chronology in this study, however, shows that the Barents Sea Ice Sheet was most likely present at the shelf edge in the Bear Island Trough for a much shorter period during the last 30 ka than

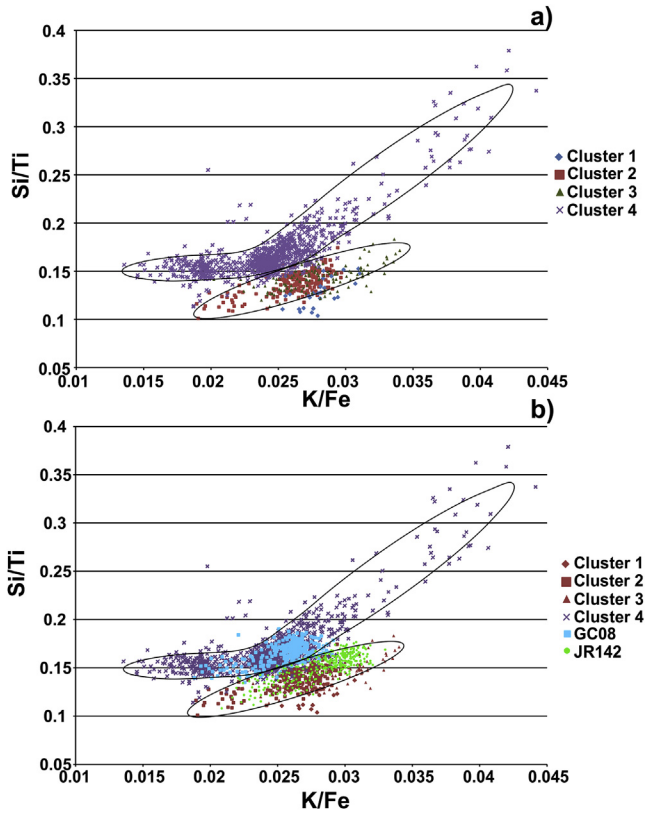


**Fig. 9.** a) Geochemical ratios of the mud fraction of the distal debris-flow deposits in core PE73. Cluster 1 includes distal debris-flow muds from the Late Weichselian. Cluster 2 includes distal debris-flow muds from between 39,400 Cal BP and 36,000 Cal BP. Cluster 3 includes distal debris-flow muds from between 68,000°BP and 60,000°BP. Cluster 4 includes distal debris-flow muds from before ~128,000°BP. b) Geochemical ratios of the distal debris-flow muds in core PE73 overlain with the same ratio data from mud fractions in GC08 and JR142. GC08 ratio data is similar to Cluster 4. JR142 ratio data is similar to Clusters 1–3.

was previously implied by the numerical modelling of Dowdeswell and Siegert (1999). The period may have only been 5.1 ka, from 26,000 to 20,900 Cal BP (Fig. 8). This is based on the assumption that the duration over which distal debris-flow muds occur is comparable to the period which ice was at the shelf edge and that there was minimal delay between glacigenic debris-flow run-out to our core sites and appearance and disappearance of the ice at the shelf edge. If these assumptions hold, then the rates of sediment supply to the shelf edge by the ice stream may have been about twice those inferred from numerical modelling. This would make the sediment supply rate twice that of the modern Amazon River.

Such high sediment-supply rates have implications for the processes of sediment deformation and advection along the submerged base of the ice stream, which themselves play a key role in ice sheet dynamics (Benn et al., 2007a, 2007b; Schoof, 2007) and are thus important to better constrain. In particular, the thickness of deforming sediment affects basal drag on the ice stream and, hence, its velocity. The Dowdeswell and Siegert (1999) model implies that the high sediment-delivery rate needed to delivery 4200 $km^3$ of sediment in 5.1 ka would require an actively deforming layer in excess of 6 m thick or an ice stream velocity greatly exceeding the 1 km $a^{-1}$ predicted in the numerical model. Modern observations of ice stream beds in Antarctica suggest, however, that deforming basal layers a number of metres in thickness are unlikely (Engelhardt and Kamb, 1998; Tulaczyk et al., 2000; Whillans et al., 2001; Dowdeswell et al., 2004).

Assuming, instead, that ~4200 $km^3$ of sediment was delivered to the Bear Island Trough-Mouth Fan over the period which distal debris-flow muds suggest ice was present at the shelf edge during the whole Weichselian suggests that the sediment accumulated over 16.5 ka (5.1 ka during MIS 2, 3.4 ka during MIS 3 and 8 ka during MIS 4). This would advocate a rate of sediment delivery of 0.25 $km^3$ $a^{-1}$ by the Bear Island Ice stream. A rate of sediment delivery of 0.25 $km^3$ $a^{-1}$ is more comparable to the modelled rates of sediment transport by Dowdeswell and Siegert (1999) and to estimates of sediment delivery made for the palaeo-ice stream draining Marguarite Bay (Dowdeswell et al., 2004). The disparity between these two scenarios makes it clear that better constraint of Bear Island Ice stream velocities and rates of bed deformation need to be made in order to improve our understanding of the Barents Sea Ice Sheet. This can only be achieved through more precise dating and correlation of sedimentary units across the entire Bear Island Trough-Mouth Fan.

#### 4.2.2. *Ice-sheet configuration*

The geochemical composition of the mud fraction of the distal debris-flow muds in cores PE73, PE75, GC08 and JR142 were analysed using ITRAX μXRF data (Fig. 9). In core PE73 there were shown to be distinct differences between the major element ratios of the distal debris-flow muds from the Weichselian glaciations and the muds from the Saalian glaciation. When these ratios were compared to ratios from other regions, the composition of the Weichselian distal debris-flow muds was found to be similar to ratio data from east of Svalbard (Figs. 1 and 9b). The composition of the Saalian distal debris-flow muds was found to be similar to ratio data from a distal debris-flow mud from the central Bear Island Trough-Mouth Fan (Fig. 9b). These findings suggest that the configuration of the Barents Sea Ice Sheet may have changed between the Saalian and the Weichselian.

The similarities in the mud geochemical compositions between distal debris-flow muds in the cores indicate a change in sediment provenance between glaciations for the northern end of the Bear Island Trough-Mouth Fan. During the Weichselian, sediment was predominantly derived from the east of Svalbard in the Barents Sea (Fig. 10a). The location of an ice dome east of Svalbard delivering ice and sediment to the Bear Island Trough is consistent with regional seafloor geomorphology and flow-direction indicators for the Last Glacial Maximum (Andreassen et al., 2008, 2014; Hogan et al., 2010; Winsborrow et al., 2010). The geochemical composition of sediment in GC08 on the central Bear Island Trough-Mouth Fan during the Last Glacial Maximum suggests a more southerly source for this sediment (Fig. 10b). Ice input to the Bear Island Trough during the Saalian may therefore have originated from an ice dome that was centred on either Scandinavia or in the central Barents Sea (Fig. 10b). The ice-sheet configuration during the Saalian could have therefore resulted in little or no ice from an ice dome east of Svalbard being drained through Bear Island Trough.

### 4.3. *Controls on ice sheet dynamics*

The importance of ocean-atmosphere-ice interactions over long timescales are indicated by contrasts between the distal debris-flow muds. The Saalian Bear Island Ice stream was possibly fed predominantly by ice from Scandinavia, or at least from a dome further south in the Barents Sea (Fig. 10b). The Weichselian Bear Island Ice stream was dominated by ice derived from east of Svalbard (Fig. 10a; Winsborrow et al., 2010, 2012; Andreassen et al., 2014). The contrasts between the two regimes are probably a result of different patterns of snow accumulation (Mangerud et al., 1998; Siegert et al., 2001). The dominance of a more southerly ice dome during the Saalian is likely due to greater accumulation

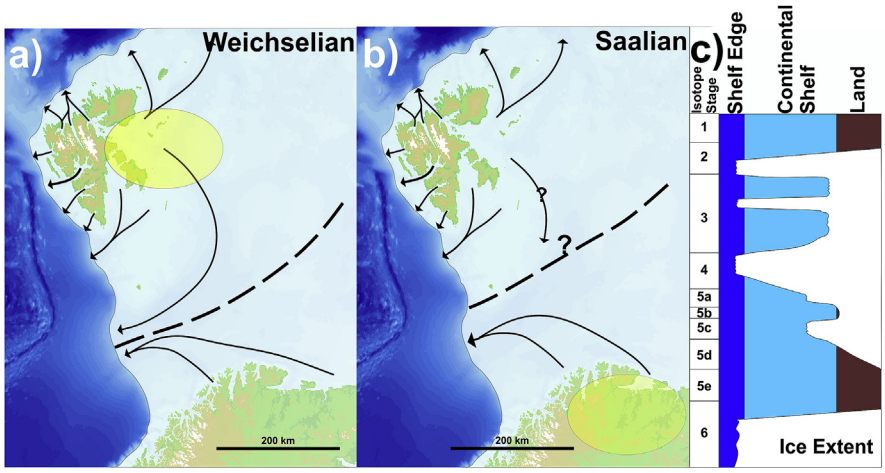


**Fig. 10.** Ice sheet chronology for the Bear Island Trough during the last 140 ka. a) Palaeo ice-flow directions during the Weichselian with respect to the Bear Island Trough-Mouth Fan. During the Weichselian the northern end of the fan is dominated by an ice dome (in yellow) east of Svalbard. b) Palaeo ice-flow directions during the Saalian glaciation. During the Saalian the northern end of the fan is dominated by an ice dome (in yellow) associated with northern Scandinavia. c) A schematic plot of glacial advance and retreat in the Bear Island Trough. Ice advances are in white, areas currently below sea level are in blue and areas currently above sea level are in brown. (For interpretation of the references to colour in this figure legend, the reader is referred to the web version of this article).

occurring further south during this time period; the difference in accumulation patterns leading to a different flow-partition pattern (Siegert and Marsiat, 2001; Bennett, 2003; Svendsen et al., 2004b; Ottesen et al., 2007).

The importance of ocean-atmosphere-ice interactions over short timescales is indicated by the timing of emplacement of the last glacigenic debris-flow deposits on the Bear Island Trough-Mouth Fan suggesting retreat prior to the global Last Glacial Maximum. Similarly early retreats from the shelf edge (~20,000 Cal BP) have also been reconstructed for ice streams offshore Svalbard (Rasmussen et al., 2007; Jessen et al., 2010; Hormes et al., 2013). On Svalbard, the cause of early thinning and retreat has been cited as possible changes to regional precipitation patterns. Biomarker proxies have been used to show an increased extent and duration of sea-ice prior to and at the Last Glacial Maximum (Müller et al., 2009; Müller and Stein, 2014). Greater sea-ice coverage would have acted to increase the distance between a possible moisture source and the ice sheet interior. In addition, atmospheric modelling has suggested a southerly shift of the Oceanic Polar Front as a consequence of topographical forcing by the Barents Sea Ice Sheet (Pausata et al., 2011). A southerly shift of the Oceanic Polar Front would reduce the number of low-pressure systems reaching Svalbard (Siegert et al., 2001). This climatic adjustment would have led to a reduction in the amount of precipitation reaching the accumulation areas of Svalbard's ice streams. Reduced precipitation would lead to glacier thinning and possible retreat from the shelf edge (Helsen et al., 2008).

Coincident retreat of the Bear Island Ice stream from the shelf edge, and ice streams from the shelf edge around Svalbard to the north, implies a consistent forcing mechanism. The climatic reorganisation suggested regionally for Svalbard, may therefore not have been limited to Svalbard but affected the interior of the Barents Sea Ice Sheet. Given the position of the ice dome feeding the Bear Island Ice stream to the east of Svalbard (Fig. 10; Hogan et al., 2010; Winsborrow et al., 2010) it is perhaps unsurprising that atmospheric forcing is similar here to that on Svalbard itself. The reduction in surface accumulation across the interior of the Barents Sea Ice Sheet is likely to be a factor in the retreat of the Bear Island Ice stream from the shelf edge and into the deeper water of the cross-shelf trough (Hebbeln et al., 1994). The early retreat into deeper water and thinning of the ice sheet interior may have made the ice sheet more sensitive to future climate and oceanic forcing as a consequence of increased calving associated with the higher buoyancy of deeper water (Benn et al., 2007a, 2007b; Amundson et al., 2010). Both factors would have enhanced the likelihood of further rapid retreat.

## 5. Conclusions

Previous work on the Barents Sea Ice Sheet has inferred four advances to the shelf edge during the past 140,000 years (Fig. 10c). The number and timing of these advances was estimated using terrestrial records and proxies for ice advance such as ice-rafted debris. This study is the first to use distal debris-flow mud layers, and thus constrain the dynamics of the Barents Sea Ice Sheet in the Bear Island Trough over the last 140,000 years. The primary conclusion of our work is that distal debris-flow muds have been emplaced during four distinct time periods and are inferred to be representative of the times when ice was at the shelf edge. The timing of these ice advances differs from reconstructions of glacial history made previously but is consistent with ice-rafted debris deposits offshore of the Bear Island Trough-Mouth Fan. The four ice advances to the shelf edge occurred between 26,000 and 20,900, 39,400 to 36,000, 68,000 to 60,000 and >128,000 years BP.

Secondly, we show that the number and thickness of distal debris-flow mud deposits associated with each ice advance differs. We suggest that this is a consequence of the stability of the ice-margin position and that it differed between the Weichselian and Saalian advances. Following the advance to the shelf edge during the Saalian, the Barents Sea Ice Sheet ice-margin was more stable and longer-lasting than any of the Weichselian advances as indicated by the thinner and less numerous distal debris-flow muds emplaced during the Weichselian.

Thirdly, we show that the geochemical composition of the distal debris-flow muds differs between the Saalian and the Weichselian. Using geochemical data from cores elsewhere around the Barents Sea, we suggest that this is a result of changing Barents Sea Ice Sheet configurations. We suggest that the Bear Island Trough drained ice predominantly from Scandinavia during the Saalian and drained ice predominantly from east of Svalbard during the Weichselian.

The results of this study indicate that deposits on trough-mouth fans can be used to reconstruct ice sheet chronologies. Specifically, it is possible to use the presence or absence of glacigenic debris-flow deposits to identify when ice is present at the shelf edge and where the ice has drained from over multiple advance and retreat cycles. Where multiple glacial advances and retreats can be identified using glacigenic debris-flow deposits, future efforts should be directed at reconstructing regional environmental variables such as sea-surface temperature and sea-ice coverage to identify whether there is any commonality of forcing associated with retreats. This may help to better understand forcing of contemporary marine-based ice masses.

## Acknowledgements

We would like to thank the editor Neil Glasser and an anonymous reviewer for their comments which greatly improved the manuscript. This research was supported by the UK NERC Arctic Research Programme under the project on whether climate change increases the landslide-tsunami risk to the UK (NE/K00008X/1; NE/K000187/1). E. Pope was supported by grant NE/K00008X/1. The crew and shipboard parties of the RV *Pelagia* and the RSS *James Clark Ross* (JCR) are thanked for their help in collection of the numerous cores involved in this project. Earlier work on the JCR was supported by NERC grant NER/T/S/2003/00318. Thanks are also given to BOSCORF and the curators S. MacLachan and M. Edwards for their services in maintaining the cores and aiding some of the analytical techniques.

## References

Amundson, J.M., Fahnestock, M., Truffer, M., Brown, J., Lüthi, M.P., Motyka, R.J., 2010. Ice mélange dynamics and implications for terminus stability, Jakobshavn Isbræ, Greenland. J. Geophys. Res. Earth Surf. 115, 2003–2012.
Andreassen, K., Laberg, J.S., Vorren, T.O., 2008. Seafloor geomorphology of the SW Barents Sea and its glaci-dynamic implications. Geomorphology 97, 157–177.
Andreassen, K., Winsborrow, M.C.M., Bjarnadóttir, L.R., Rüther, D.C., 2014. Ice stream retreat dynamics inferred from an assemblage of landforms in the northern Barents Sea. Quat. Sci. Rev. 92, 246–257.
Backman, J., Fornaciari, E., Rio, D., 2009. Biochronology and paleoceanography of late Pleistocene and Holocene calcareous nannofossil abundances across the Arctic Basin. Mar. Micropaleontol. 72, 86–98.
Barkoulas, J.T., Baum, C.F., Travlos, N., 2000. Long memory in the Greek stock market. Appl. Financ. Econ. 10, 177–184.
Batchelor, C., Dowdeswell, J., 2014. The physiography of High Arctic cross-shelf troughs. Quat. Sci. Rev. 92, 68–96.
Benn, D.I., Hulton, N.R.J., Mottram, R.H., 2007a. 'Calving laws','sliding laws' and the stability of tidewater glaciers. Ann. Glaciol. 46, 123–130.
Benn, D.I., Warren, C.R., Mottram, R.H., 2007b. Calving processes and the dynamics of calving glaciers. Earth-Sci. Rev. 82, 143–179.
Bennett, M.R., 2003. Ice streams as the arteries of an ice sheet: their mechanics, stability and significance. Earth-Sci. Rev. 61, 309–339.
Chen, C., Hiscott, R.N., 1999. Statistical analysis of facies clustering in submarine-fan turbidite successions. J. Sediment. Res. 69, 505–517.
Cheshire, H., Thurow, J., Nederbragt, A.J., 2005. Late Quaternary climate change record from two long sediment cores from Guaymas Basin, Gulf of California. J. Quat. Sci. 20, 457–469.
Clare, M.A., Talling, P.J., Challenor, P., Malgesini, G., Hunt, J.E., 2014. Distal turbidites reveal a common distribution for large (>0.1 $km^3$) submarine landslide recurrence. Geology 42, 263–266.
Colleoni, F., Krinner, G., Jakobsson, M., Peyaud, V., Ritz, C., 2009. Influence of regional parameters on the surface mass balance of the Eurasian ice sheet during the peak Saalian (140 kya). Glob. Planet. Change 68, 132–148.
Croudace, I.W., Rindby, A., Rothwell, R.G., 2006. ITRAX: description and evaluation of a new multi-function x-ray core scanner. Geol. Soc. Lond. 267, 51. Special publication.
Dowdeswell, J.A., Elverhøi, A., 2002. The timing of initiation of fast-flowing ice streams during a glacial cycle inferred from glacimarine sedimentation. Mar. Geol. 188, 3–14.
Dowdeswell, J.A., Elverhøi, A., Andrews, J.T., Hebbeln, D., 1999. Asynchronous deposition of ice-rafted layers in the Nordic seas and North Atlantic Ocean. Nature 400, 348–351.
Dowdeswell, J.A., Elverhoi, A., Spielhagen, R., 1998. Glacimarine sedimentary processes and facies on the Polar North Atlantic margins. Quat. Sci. Rev. 17, 243–272.
Dowdeswell, J.A., Ó Cofaigh, C., Pudsey, C.J., 2004. Thickness and extent of the subglacial till layer beneath an Antarctic paleo–ice stream. Geology 32, 13–16.
Dowdeswell, J.A., Ottesen, D., Rise, L., 2010. Rates of sediment delivery from the Fennoscandian Ice Sheet through an ice age. Geology 38, 3–6.
Dowdeswell, J.A., Siegert, M.J., 1999. Ice-sheet numerical modeling and marine geophysical measurements of glacier-derived sedimentation on the Eurasian Arctic continental margins. Geol. Soc. Am. Bull. 111, 1080–1097.
Dreger, D., 1999. Decadal to Centennial Scale Sediment Records of Ice Advance on the Barents Shelf and Meltwater Discharge into the Northeastern Norwegian Sea over the Last 40 Kyr: dekadische Bis Jahrhundert-Variabilität Von Eisvorstößen Auf Dem Barentsschelf und Schmelzwasserschüben in Die Nordöstliche Norwegensee Während Der Letzten 40 Ka. Inst. für Geowiss, pp. 1–79.
Ehlers, J., Gibbard, P.L., 2004. Quaternary Glaciations-extent and Chronology: Part I: Europe. Elsevier.
Elverhoi, A., Andersen, E.S., Dokken, T., Hebbeln, D., Spielhagen, R., Svendsen, J.I., Sorflaten, M., Rornes, A., Hald, M., Forsberg, C.F., 1995. The growth and decay of the late weichselian ice sheet in western Svalbard and adjacent areas based on provenance studies of marine sediments. Quat. Res. 44, 303–316.
Engelhardt, H., Kamb, B., 1998. Basal sliding of ice stream B, West Antarctica. J. Glaciol. 44, 223–230.
Gard, G., 1988. Late Quaternary calcareous nannofossil biozonation, chronology and palaeo-oceanography in areas north of the Faeroe-Iceland Ridge. Quat. Sci. Rev. 7, 65–78.
Hebbeln, D., Dokken, T., Andersen, E.S., Hald, M., Elverhøi, A., 1994. Moisture supply for northern ice-sheet growth during the last glacial maximum. Nature 370, 357–360.
Helsen, M.M., van den Broeke, M.R., van de Wal, R.S.W., van de Berg, W.J., van Meijgaard, E., Davis, C.H., Li, Y., Goodwin, I., 2008. Elevation changes in Antarctica mainly determined by accumulation variability. Science 320, 1626–1629.
Hibbert, F.D., Austin, W.E.N., Leng, M.J., Gatliff, R.W., 2010. British Ice Sheet dynamics inferred from North Atlantic ice-rafted debris records spanning the last 175,000 years. J. Quat. Sci. 25, 461–482.
Hogan, K.A., Dowdeswell, J.A., Noormets, R., Evans, J., Cofaigh, C.Ó., 2010. Evidence for full-glacial flow and retreat of the Late Weichselian Ice Sheet from the waters around Kong Karls Land, eastern Svalbard. Quat. Sci. Rev. 29, 3563–3582.
Hormes, A., Gjermundsen, E.F., Rasmussen, T.L., 2013. From mountain top to the deep sea–Deglaciation in 4D of the northwestern Barents Sea Ice Sheet. Quat. Sci. Rev. 75, 78–99.
Hughes, A.L.C., Gyllencreutz, R., Lohne, Ø.S., Mangerud, J., Svendsen, J.I., 2016. The last Eurasian ice sheets–a chronological database and time-slice reconstruction, DATED-1. Boreas 45, 1–45.
Hunt, J.E., Wynn, R.B., Talling, P.J., Masson, D.G., 2013. Frequency and timing of landslide-triggered turbidity currents within the Agadir Basin, offshore NW Africa: are there associations with climate change, sea level change and slope sedimentation rates? Mar. Geol. 346, 274–291.
Hurst, H.E., 1951. Long-term storage capacity of reservoirs. Trans. Amer. Soc. Civ. Eng. 116, 770–808.
Ingólfsson, Ó., Landvik, J.Y., 2013. The Svalbard–Barents Sea ice-sheet–Historical, current and future perspectives. Quat. Sci. Rev. 64, 33–60.
Jessen, S.P., Rasmussen, T.L., Nielsen, T., Solheim, A., 2010. A new Late Weichselian and Holocene marine chronology for the western Svalbard slope 30,000–0 Cal years BP. Quat. Sci. Rev. 29, 1301–1312.
Knies, J., Kleiber, H.-P., Matthiessen, J., Müller, C., Nowaczyk, N., 2001. Marine ice-rafted debris records constrain maximum extent of Saalian and Weichselian ice-sheets along the northern Eurasian margin. Glob. Planet. Change 31, 45–64.
Laberg, J.S., Dowdeswell, J.A., 2016. Glacigenic debris-flows on the Bear Island trough-mouth fan, Barents Sea margin. In: Dowdeswell, J.A., Canals, M., Jakobsson, M., Todd, B.J., Dowdeswell, E.K., Hogan, K.A. (Eds.), Atlas of Submarine Glacial Landforms: Modern, Quaternary and Ancient, vol. 46. Geological Society, London, Memoirs.
Laberg, J.S., Vorren, T.O., 1995. Late Weichselian submarine debris flow deposits on the Bear Island Trough mouth fan. Mar. Geol. 127, 45–72.
Laberg, J.S., Vorren, T.O., 1996. The middle and late Pleistocene evolution and the Bear Island trough mouth fan. Glob. Planet. Change 12, 309–330.
Labeyrie, L.D., Duplessy, J.C., 1985. Changes in the oceanic 13 C/12 C ratio during the last 140,000 years: high-latitude surface water records. Palaeogeogr. Palaeoclimatol. Palaeoecol. 50, 217–240.
Lambeck, K., Purcell, A., Zhao, J., Svensson, N.O., 2010. The Scandinavian ice sheet: from MIS 4 to the end of the Last Glacial maximum. Boreas 39, 410–435.
Landvik, J.Y., Bondevik, S., Elverhøi, A., Fjeldskaar, W., Mangerud, J., Salvigsen, O., Siegert, M.J., Svendsen, J.-I., Vorren, T.O., 1998. The last glacial maximum of Svalbard and the Barents Sea area: ice sheet extent and configuration. Quat. Sci. Rev. 17, 43–75.
Lebreiro, S.M., Voelker, A.H.L., Vizcaino, A., Abrantes, F.G., Alt-Epping, U., Jung, S., Thouveny, N., Gracia, E., 2009. Sediment instability on the Portuguese continental margin under abrupt glacial climate changes (last 60 kyr). Quat. Sci. Rev. 28, 3211–3223.
Lucchi, R.G., Camerlenghi, A., Rebesco, M., Colmenero-Hidalgo, E., Sierro, F.J., Sagnotti, L., Urgeles, R., Melis, R., Morigi, C., Bárcena, M.-A., 2013. Postglacial sedimentary processes on the Storfjorden and Kveithola trough mouth fans: significance of extreme glacimarine sedimentation. Glob. Planet. Change 111, 309–326.
Mandelbrot, B.B., Van Ness, J.W., 1968. Fractional Brownian motions, fractional

noises and applications. SIAM Rev. 10, 422–437.
Mangerud, J., Astakhov, V.I., Murray, A., Svendsen, J.I., 2001. The chronology of a large ice-dammed lake and the Barents–Kara Ice Sheet advances, Northern Russia. Glob. Planet. Change 31, 321–336.
Mangerud, J., Dokken, T., Hebbeln, D., Heggen, B., Ingolfsson, O., Landvik, J.Y., Mejdahl, V., Svendsen, J.I., Vorren, T.O., 1998. Fluctuations of the Svalbard–Barents Sea Ice Sheet during the last 150,000 years. Quat. Sci. Rev. 17, 11–42.
Milliman, J.D., Syvitski, J.P.M., 1992. Geomorphic Tectonic control of sediment discharge to the Ocean – the importance of small mountainous rivers. J. Geol. 100, 525–544.
Müller, J., Massé, G., Stein, R., Belt, S.T., 2009. Variability of sea-ice conditions in the Fram Strait over the past 30,000 years. Nat. Geosci. 2, 772–776.
Müller, J., Stein, R., 2014. High-resolution record of late glacial and deglacial sea ice changes in Fram Strait corroborates ice–ocean interactions during abrupt climate shifts. Earth Planet. Sci. Lett. 403, 446–455.
Nygard, A., Sejrup, H.P., Haflidason, H., Bryn, P., 2005. The glacial North Sea Fan, southern Norwegian Margin: architecture and evolution from the upper continental slope to the deep-sea basin. Mar. Pet. Geol. 22, 71–84.
Nygård, A., Sejrup, H.P., Haflidason, H., Lekens, W.A.H., Clark, C.D., Bigg, G.R., 2007. Extreme sediment and ice discharge from marine-based ice streams: new evidence from the North Sea. Geology 35, 395–398.
Ó Cofaigh, C., Taylor, J., Dowdeswell, J.A., Pudsey, C.J., 2003. Palaeo-ice streams, trough mouth fans and high-latitude continental slope sedimentation. Boreas 32, 37–55.
Ottesen, D., Dowdeswell, J.A., Landvik, J.Y., Mienert, J., 2007. Dynamics of the Late Weichselian ice sheet on Svalbard inferred from high-resolution sea-floor morphology. Boreas 36, 286–306.
Ottesen, D., Dowdeswell, J.A., Rise, L., 2005. Submarine landforms and the reconstruction of fast-flowing ice streams within a large Quaternary ice sheet: the 2500 km-long Norwegian-Svalbard margin (57–80 N). Geol. Soc. Am. Bull. 117, 1033–1050.
Patton, H., Andreassen, K., Bjarnadóttir, L.R., Dowdeswell, J.A., Winsborrow, M.C.M., Noormets, R., Polyak, L., Auriac, A., Hubbard, A., 2015. Geophysical constraints on the dynamics and retreat of the Barents Sea Ice Sheet as a palaeo-benchmark for models of marine ice-sheet deglaciation. Rev. Geophys. 53, 1051–1098.
Pausata, F.S.R., Li, C., Wettstein, J., Kageyama, M., Nisancioglu, K.H., 2011. The key role of topography in altering North Atlantic atmospheric circulation during the last glacial period. Clim. Past 7, 1089–1101.
Pope, E.L., Talling, P.J., Urlaub, M., Hunt, J.E., Clare, M.A., Challenor, P., 2015. Are large submarine landslides temporally random or do uncertainties in available age constraints make it impossible to tell? Mar. Geol. 369, 19–33.
Rasmussen, T.L., Thomsen, E., Ślubowska, M.A., Jessen, S., Solheim, A., Koç, N., 2007. Paleoceanographic evolution of the SW Svalbard margin (76 N) since 20,000 14 C yr BP. Quat. Res. 67, 100–114.
Reimer, P.J., Bard, E., Bayliss, A., Beck, J.W., Blackwell, P.G., Ramsey, C.B., Buck, C.E., Cheng, H., Edwards, R.L., Friedrich, M., 2013. IntCal13 and Marine13 radiocarbon age calibration curves 0–50,000 years Cal BP. Radiocarbon 55, 1869–1887.
Richter, T.O., Lassen, S., van Weering, T.C.E., De Haas, H., 2001. Magnetic susceptibility patterns and provenance of ice-rafted material at Feni Drift, Rockall Trough: implications for the history of the British–Irish ice sheet. Mar. Geol. 173, 37–54.
Rothwell, R.G., Hoogakker, B., Thomson, J., Croudace, I.W., Frenz, M., 2006. Turbidite emplacement on the Southern Balearic Abyssal Plain (Western Mediterranean Sea) during Marine Isotope Stages 1–3: an application of ITRAX XRF scanning of sediment cores to lithostratigraphic analysis. Geol. Soc. Lond. 267, 79–98. Special Publications.
Sættem, J., Bugge, T., Fanavoll, S., Goll, R.M., Mørk, A., Mørk, M.B.E., Smelror, M., Verdenius, J.G., 1994. Cenozoic margin development and erosion of the Barents Sea: core evidence from southwest of Bjørnøya. Mar. Geol. 118, 257–281.
Schoof, C.G., 2007. Ice sheet grounding line dynamics: steady states, stability, and hysteresis. J. Geophys. Res. Earth Surf. 112, 2003–2012.
Siegert, M.J., Dowdeswell, J.A., Hald, M., Svendsen, J.-I., 2001. Modelling the Eurasian Ice Sheet through a full (Weichselian) glacial cycle. Glob. Planet. Change 31, 367–385.
Siegert, M.J., Marsiat, I., 2001. Numerical reconstructions of LGM climate across the Eurasian Arctic. Quat. Sci. Rev. 20, 1595–1605.
Solheim, A., Faleide, J.I., Andersen, E.S., Elverhøi, A., Forsberg, C.F., Vanneste, K., Uenzelmann-Neben, G., Channell, J.E.T., 1998. Late Cenozoic seismic stratigraphy and glacial geological development of the East Greenland and Svalbard–Barents Sea continental margins. Quat. Sci. Rev. 17, 155–184.
Solignac, S., Seidenkrantz, M.-S., Jessen, C., Kuijpers, A., Gunvald, A.K., Olsen, J., 2011. Late-Holocene sea-surface conditions offshore Newfoundland based on dinoflagellate cysts. Holocene 21, 539–552.
Spielhagen, R.F., Baumann, K.-H., Erlenkeuser, H., Nowaczyk, N.R., Nørgaard-Pedersen, N., Vogt, C., Weiel, D., 2004. Arctic Ocean deep-sea record of northern Eurasian ice sheet history. Quat. Sci. Rev. 23, 1455–1483.
Svendsen, J.I., Alexanderson, H., Astakhov, V.I., Demidov, I., Dowdeswell, J.A., Funder, S., Gataullin, V., Henriksen, M., Hjort, C., Houmark-Nielsen, M., 2004a. Late Quaternary ice sheet history of northern Eurasia. Quat. Sci. Rev. 23, 1229–1271.
Svendsen, J.I., Astakhov, V.I., Bolshiyanov, D.Y., Demidov, I., Dowdeswell, J.A., Gataullin, V., Hjort, C., Hubberten, H.W., Larsen, E., Mangerud, J., 1999. Maximum extent of the Eurasian ice sheets in the Barents and Kara Sea region during the Weichselian. Boreas 28, 234–242.
Svendsen, J.I., Gataullin, V., Mangerud, J., Polyak, L., 2004b. The glacial history of the Barents and Kara Sea region. Dev. Quat. Sci. 2, 369–378.
Taylor, J., Dowdeswell, J.A., Kenyon, N.H., Ó Cofaigh, C., 2002a. late quaternary architecture of trough-mouth fans: Debris flows and suspended sediments on the Norwegian Margin. Geol. Soc. Lond. 203, 55–71. Special Publications.
Taylor, J., Dowdeswell, J.A., Siegert, M.J., 2002b. Late Weichselian depositional processes, fluxes, and sediment volumes on the margins of the Norwegian Sea (62–75 N). Mar. Geol. 188, 61–77.
Tulaczyk, S., Kamb, W.B., Engelhardt, H.F., 2000. Basal mechanics of Ice Stream B, west Antarctica: 2. Undrained plastic bed model. J. Geophys. Res. Solid Earth 105, 483–494.
Vogt, C., Knies, J., Spielhagen, R.F., Stein, R., 2001. Detailed mineralogical evidence for two nearly identical glacial/deglacial cycles and Atlantic water advection to the Arctic Ocean during the last 90,000 years. Glob. Planet. Change 31, 23–44.
Vorren, T.O., Laberg, J.S., 1997. Trough mouth fans—palaeoclimate and ice-sheet monitors. Quat. Sci. Rev. 16, 865–881.
Vorren, T.O., Laberg, J.S., Blaume, F., Dowdeswell, J.A., Kenyon, N.H., Mienert, J., Rumohr, J., Werner, F., 1998. The Norwegian Greenland Sea continental margins: morphology and late Quaternary sedimentary processes and environment. Quat. Sci. Rev. 17, 273–302.
Vorren, T.O., Landvik, J.Y., Andreassen, K., Laberg, J.S., 2011. Glacial history of the Barents Sea region. Quaternary Glaciations—Extent and chronology—a closer look. Dev. Quat. Sci 361–372.
Vorren, T.O., Richardsen, G., Knutsen, S.-M., Henriksen, E., 1991. Cenozoic erosion and sedimentation in the western Barents Sea. Mar. Pet. Geol. 8, 317–340.
Weaver, P.P.E., Kuijpers, A., 1983. Climatic Control of Turbidite Deposition on the Madeira Abyssal Plain.
Weaver, P.P.E., Rothwell, R.G., Ebbing, J., Gunn, D., Hunter, P.M., 1992. Correlation, frequency of emplacement and source directions of megaturbidites on the Madeira Abyssal Plain. Mar. Geol. 109, 1–20.
Wetzel, A., 1984. Bioturbation in deep-sea fine-grained sediments: influence of sediment texture, turbidite frequency and rates of environmental change. Geol. Soc. Lond. 15, 595–608. Special Publications.
Whillans, I.M., Bentley, C.R., Van der Veen, C.J., 2001. Ice Streams B and C. The West Antarctic Ice Sheet: Behavior and Environment, pp. 257–281.
Winsborrow, M.C.M., Andreassen, K., Corner, G.D., Laberg, J.S., 2010. Deglaciation of a marine-based ice sheet: Late Weichselian palaeo-ice dynamics and retreat in the southern Barents Sea reconstructed from onshore and offshore glacial geomorphology. Quat. Sci. Rev. 29, 424–442.
Winsborrow, M.C.M., Stokes, C.R., Andreassen, K., 2012. Ice-stream flow switching during deglaciation of the southwestern Barents Sea. Geol. Soc. Am. Bull. 124, 275–290.